Received March 15, 2020, accepted April 15, 2020, date of publication May 11, 2020

Semi-automatic 3-D Reconstruction Measurement of Muscle Volume with Magnetic Resonance Imaging

By Q. Zhou, Q. Hu, X. Yang, Y. Chen, Y. Yu, J. Zhang, Q. Ma, G. Zhou, H. Wei, B. Zhang, H. Zhang

Department of Radiology, The affiliated Jiangning hospital of Nanjing medical university, No.168, gushan Road, Nanjing, Jiangsu Province, China

ABSTRACT

Background and Objective

We aimed to assess and verify the measurement accuracy and feasibility of semi-automatic magnetic resonance imaging (MRI) volume of interest (VOI) method by comparing its measurements with actual skeletal muscle volumes and discuss the clinical significance.

Material and Methods

A total of 18 muscles from 2 pigs were measured by drainage method, VOI method (VVOI), the summation method (Vsum), and maximum section method (Vmax) respectively after MRI scanning. All measurements were performed by 2 musculoskeletal radiologists and repeated at 6 different times, recording the consuming time (minutes) of every muscle. The average result of the 2 radiologists was adopted.

Results

The 3-D structure of the skeletal muscles was distinct and vivid. A Friedman test and the inter-class correlation coefficient (ICC) indicated the VOI method had a high intra- and inter-reliability. The root mean square error (RMSE) over 6 time-points was 1.101 mL. A Bland-Altman plot represented a superior consistency. Pairwise Mann–Whitney U testing demonstrated that the consuming time to measure each muscle by VOI method was short.

Conclusions

The VOI method could semi-automatically display the 3-D reconstruct of the skeletal muscle clearly, conveniently, with a great accuracy, and high repeatability.

Keywords – *Magnetic Resonance Imaging; Skeletal Muscle; Dimensional Measurement Accuracy; muscular atrophy; Pigs.*

INTRODUCTION

Age-related degeneration and some diseases can change skeletal muscle volume,[1,2] especially in the upper limbs.[3] As the volume of muscle determines the maximal muscle force it can generate,[4] upper limb muscle atrophy can lead to instability of the shoulder joint, causing secondary joint damage, physical disability, persistent arthralgia, and dysfunction.[5–7] The volume of muscle is a predictor of poor outcomes, including mortality, disability, and poor quality of life.[8] On the other hand, its morphological change is an important indicator for the development of competitive sports training programs, clinical evaluations, and research observation in orthopedics and sports medicine.[9–11] Given

the above, quantifying these features of the upper limb is important for providing context for healthy aging, musculoskeletal disorders, and is a functioning indicator whenever they occur in old or young patients.

Magnetic resonance imaging (MRI) plays an important role in evaluating muscle volume and displaying 3-D structure.[12] Previous studies have reported the MRI 3-D reconstruction and volume measurement by delineating the contour manually.4,[12–15] However, the manual operation was tedious and less reproducible. In methods such as deformation of a parametric specific object, the mean time for reconstruction was one hour.[4] It has been reported that the volume of interest (VOI) method, a semi-automatic measurement based on routine MRI, can detect age-related degeneration and rotator cuff tear by measuring the deltoid muscle volume conveniently and directly.[16] However, the accuracy and feasibility of the VOI method had not been verified, especially when its measurements were compared to the actual muscle volumes.

Considering that it is unrealizable to compare the measurements with the actual muscle volumes of the living human body, the ethical problems and limited availability of cadaveric specimens rarely has research on human corpses been reported.[17–19] Nevertheless, an animal model can easily solve the ethical problems and frozen tissue inactivation,[20] and swine have proven to be an excellent alternative for practicing and simulating surgical strategies that cannot be performed on human cadavers.[21,22] Therefore, the primary purpose of this study was to evaluate the accuracy and repeatability of MRI VOI method by comparing the data measured by VOI with the actual forelimbs' muscle volumes of pigs. We hypothesized that the VOI method was accurate and reliable for measuring skeletal muscle volumes, and could provide a convenient and non-invasive way for clinical evaluation of sarcopenia or in orthopedics and sports medicine.

MATERIAL AND METHODS

Experimental Subject

The pig forelimbs for experiment 2 adult middle-aged female domestic pigs were bought from a pig farm where they were reared and slaughtered. The Animal Ethics Committee was provided with a waiver by our research ethics board. The 2 left forelimbs were transported to our hospital and received an MRI scan immediately after slaughtering. The period between slaughter and MRI scan was approximately 40 minutes. Freshness was maintained at 4° in transportation. We marked these 2 left forelimbs as pig forelimb 1 (PF 1, weight: 3.54Kg) and pig forelimb 2 (PF 2, weight: 3.40Kg).

MRI Scan

MRI procedures were performed with a 3.0T MRI scanner (Ingenia, Philips, Eindhoven, the Netherlands) using an16-channel Torso Coil. These 2 left forelimbs underwent the standard general clinical MRI protocol at our institution. T1-weighted turbo spin echo (TSE) imaging in the axial: repetition time (TR) = 627.0 ms, echo time (TE) = 20 ms, slice thickness = 3 mm, interlamellar space = 0.3 mm, number of excitations = 1, matrix size = 464 × 459; field of view (FOV) = 240 × 240 (mm), and the acquisition time of this sequence was 6 minutes and 24 seconds.

Drainage Method

After the MRI scanning, the 2 left forelimbs were dissected immediately by 2 orthopedics doctors. Nine muscles were dissected from each skeleton, including extensor carpi radialis/ulnaris (ECR/ECU), extensor digitorum communis (EDC), flexor digitorum profundus caput humeral/ulnare (FDPCH/FDPCU), flexor carpi radialis/ulnaris (FCR/FCU), flexor digitorum superficialis (FDS), and pronator teres (PT)23 Care was taken to ensure the entire muscle was removed from the skeleton. After dissection, excess connective tissue, tendons and fat were removed from the entire muscle. A total of 18 muscles are shown in Figure 1.

The actual volumes (Vact) of 18 muscles were measured by the drainage method. Figure 2 shows the detailed process. Vact was defined as the actual volume of the muscles. All readings were executed independently and high-resolution photos were taken horizontally by one of the musculoskeletal attending physicians. After the drainage test we checked the results with amplifying photos (Figure 2C), if inconsistent, the ultima Vact of muscle was determined by the high-resolution photos.

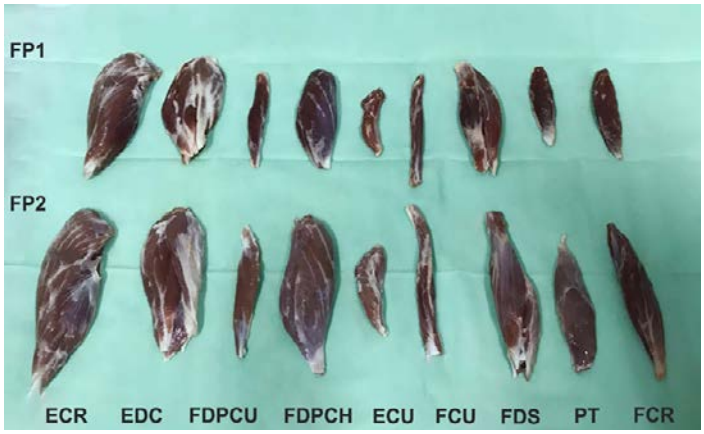

FIGURE 1. A total of 18 muscles were placed on the operating table. The 9 muscles of the PF1 were displayed in the upper row, and the lower row placed the muscles of the PF2.
ECR = extensor carpi radialis; EDC = extensor digitorum communis; ECU = extensor carpi ulnaris; FDPCH = flexor digitorum profundus caput humerale; FDPCU = flexor digitorum profundus caput ulnare; FCU = flexor carpi ulnaris; FDS = flexor digitorum superficialis; FCR = flexor carpi radialis; PT = pronator teres; PF 1 = pig forelimb 1; PF 2 = pig forelimb 2.

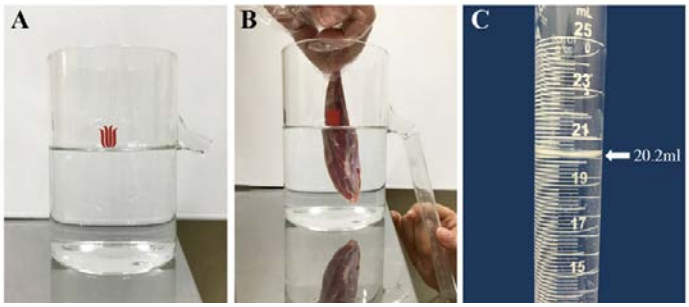

FIGURE 2. **A.** Water was placed in a custom-made cylinder, waiting until the water does not flow out. **B.** The pronator teres was put into the cylinder cautiously and a small-scale graduated cylinder was used to measure the volume of water flowing from the cylinder. **C.** The lowest scale of the crescent was read horizontally and a high-resolution photo was taken to record the scale. The actual volume of pronator teres was 20.2 mm^3.

Segmentation Principle of the VOI Method

A semi-automatic method to measure the muscle was applied (VOI method software uMR_770, united imaging healthcare, shanghai, China), which was still investigational. The algorithmic steps of the volume calculating method are presented in a compact form by the following:

a. Given the contours in slices that had been delineated, contours in intermediate slices were calculated using shaped-based interpolation to maintain continuous transition.

1. Calculate the mask from the contour in slices and specify 1 inside the contour, while 0 outside.
2. Convert the mask into a gray-value image through a distance function.[24]
3. Estimate the contour in intermediate slices by interpolating the distance-representing gray-value slices and thresholding at zero.[25]

b. A horizontal scan line algorithm is applied to calculate the internal area of the contour. For each scan line:

1. Find the intersections of the scan line with all edges of the polygon.
2. Sort the intersections by increasing x coordinate.
3. Find all pixels between pairs of intersections.

As the calculation of intersections was slow, edge coherence was considered to avoid unnecessary calculation, therefore Active Edge Table was adopted to store active edges related to the current scanline. The contour brings some ambiguity inevitably on whether the pixels should be treated as the interior of the polygon or not. Our criteria are that only pixels whose centers are interior to the polygon are counted. Therefore, the maximum error equals +/– the circumference of the contour multiplied by (largest pixel dimension) 2/2. To raise measurement accuracy, GUI (Graphical User Interface) and images are zoomed in to diminish ambiguousness.

c. The total areas were an accumulation of the areas in each slice. The volume equals the product of the accumulated area and the distance between the 2 slices' center. The volume of a VOI was the product of the spacing (normally the distance between 2 slices' center) and the accumulated area of the VOI projected in each slice.

Image processing by VOI method

The axial T1-weighted TSE images of the 2 left forelimbs were passed to the local workstation, then the VOI method software was performed to reconstruct the skeletal muscle morphology of the pig forelimb and the volume of each muscle was individually measured semi-automatically. One

musculoskeletal attending physician and one musculoskeletal associate chief physician respectively identified every skeletal muscle and contour of the muscle. Only the first/last slice, as well as the slice where the morphogenesis changes need to be delineated manually. The 3-D shape of every muscle was reconstructed and the volume was output automatically. The 2 operators repeated the above image processing 6 times every few days and recorded the entire process time (minutes). The average volume measured by these operators were taken as the result of the VOI method volume (V_{vol}).

Volume Measurement by Conventional Method

Two musculoskeletal physicians measured all the 18 muscles by the conventional method in picture archiving and communication system. The summation method volume (V_{sum}) showed the individual slice volumes, and is shown in Equation 1. The maximum section method volume (V_{max}) was the largest interface to calculate the volume is shown in Equation 2.

$$V_{sum} = \sum_{1}^{n} \alpha (l + i) \qquad \text{Equation 1}$$

$$V_{max} = \frac{\alpha_{max} (l + i) n\pi}{6} \qquad \text{Equation 2}$$

where α was the area per slice, α_{max} was the area of the maximum section, l was the slice thickness, i was the interlamellar space, and n was the number of slices. Repeated measuring 6 times at different times, record the measurements and the consuming time (minutes) of every muscle, adopt the average of the 2 physicians as the result.

Statistical analysis

Measurement data that conforms to a normal distribution were reported as mean ± standard deviation if not median was adopted. The intra-reliability in different time points were evaluated by Friedman test and inter-class correlation coefficient (ICC) was employed to evaluate the reliability of measurements between the 2 physicians. A Kruskal-Wallis H test was performed to compare the volumes and consume times in different measurement methods. Root mean square error (RMSE) was expressed as the difference between the 3 methods and the actual value. A Bland-Altman plot was applied to the data to display the distribution of measurements by various methods. A P value < 0.05 was considered statistically significant. Statistical analyses were performed with SPSS software version 21.0 (International Business Machines Corporation, Chicago Illinois, United States) and R program 3.5.0 with calculation of a two-sided P value. All graphics were created using GraphPad Prism version 5.00 for Windows (GraphPad Software, San Diego California, United States).

RESULTS

3-D Reconstruction

The morphological structure and 3-D configuration of pig forelimbs from the reconstruction of MRI VOI method was distinct and vivid (Figure 3), with a high-resolution and was consistent with the known anatomy.

Measurement Repeatability Verification

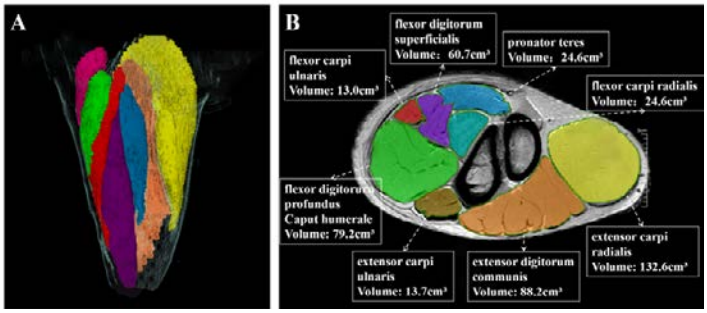

FIGURE 3. A. The morphological structure and 3-D configuration of pig forelimbs from the reconstruction of MRI VOI method was distinct and vivid. B. The cross-section images displayed different muscles using different colors and their volumes showed up automatically.

A total of 18 pig forelimb muscles were measured 6 times by 2 physicians using the MRI VOI method (Table 1 and Table 2). A Friedman test showed the mean rank of all the 6 measurements had no statistical difference (χ^2 = 1.396, P = 0.925; χ^2 = 9.38, P = 0.095, respectively), so there was a good reproducibility at different time points for one observer. The ICC value calculated from the mean measurement over all time points for each observer was close to 1 (ICC=0.999, 95% CI: 0.998~1.000). The above results indicated that the MRI VOI method demonstrated a high intra- and inter-reliability and good repeatability of volume measurements.

TABLE 1. The Volumes of 18 Muscles Measured Using VOI Method 6 Times By One Musculoskeletal Attending Physician and the Results of a Friedman Test

Muscles	Volumes (PF 1/PF 2, mm^3)						mean	χ^2	P value
	1	2	3	4	5	6			
ECR	123.3/132.6	125.6/130.4	120.8/132.3	125.5/136.5	124.7/134.4	124.9/131.8	124.13/133.0	1.396	0.925
EDC	82.7/88.2	81.5/89.6	84.7/89.2	81.4/92.1	83.8/90.5	80.1/88.4	82.36/89.67		
ECU	12.5/13.7	11.6/13.2	12.3/12.8	13.8/12.84	12.8/13.2	12.9/13.7	12.65/13.24		
FDPCH	63.57/79.2	63.5/78.6	62.4/82.3	66.7/81.4	62.2/83.5	64.8/79.5	63.86/80.75		
FDPCU	12.8/15.2	12.6/15.3	11.5/15.8	12.6/15.0	13.5/14.9	13.7/15.7	12.78/15.32		
FCU	9.5/13	9.8/13.2	10.8/12.4	10.4/13.6	10.6/13.3	10.9/12.9	10.33/13.07		
FDS	65.9/60.7	62.8/59.3	64.6/61.3	66.3/59.4	62.6/59.6	64.2/59.1	64.40/59.90		
FCR	13.8/16.9	14.2/16.4	15.6/16.7	13.8/15.4	15.3/15.9	13.5/15.7	14.36/16.16		
PT	17.7/24.6	18.1/24.7	19.5/24.1	18.7/23.4	19.6/24.3	18.2/25.1	18.63/24.37		

ECR = extensor carpi radialis; EDC = extensor digitorum communis; ECU = extensor carpi ulnaris; FDPCH = flexor digitorum profundus caput humerale; FDPCU = flexor digitorum profundus caput ulnare; FCU = flexor carpi ulnaris; FDS = flexor digitorum superficialis; FCR = flexor carpi radialis; PT = pronator teres; PF 1 = pig forelimb 1; PF 2 = pig forelimb 2.

TABLE 2. The Volumes of 18 Muscles Measured Using VOI Method 6 Times By One Musculoskeletal Associate Chief Physician and the Results of a Friedman Test

Muscles	Volumes (PF 1/PF 2, mm^3)						mean	χ^2	P value
	1	2	3	4	5	6			
ECR	124.6/130.8	125.8/131.6	125.3/135.4	122.7/133.66	125.1/134.5	124.6/134.8	124.96/133.45	9.38	0.095
EDC	84.6/87.6	86.7/88.7	87.2/86.5	86.9/88.4	85.3/88.9	84.6/89.3	85.95/88.23		
ECU	12.6/12.4	12.7/12.7	12.4/10.0	12.3/11.9	11.9/12.4	13.2/11.9	12.53/11.88		
FDPCH	66.2/77.7	65.4/78.3	67.8/79.31	66.9/78.4	64.8/77.3	65.5/78.3	65.92/78.22		
FDPCU	13.7/15.6	14.6/15.3	14.5/16.71	13.8/14.5	14.2/15.8	13.4/16.2	13.95/15.69		
FCU	10.9/12.5	10.6/12.4	10.7/13.55	11.3/11.7	10.8/12.2	10.9/11.9	11.25/12.38		
FDS	61.9/58.3	62.4/58.4	63.2/61.25	62.8/57.3	61.6/57.6	62.4/57.7	62.42/58.43		
FCR	14.8/16.9	15.2/16.8	15.3/15.88	14.7/16.3	15.7/16.5	15.6/16.5	15.28/16.48		
PT	18.5/24.4	19.3/24.6	18.4/22.74	19.2/24.5	18.5/23.8	18.6/24.3	18.93/24.06		

ECR = extensor carpi radialis; EDC = extensor digitorum communis; ECU = extensor carpi ulnaris; FDPCH = flexor digitorum profundus caput humerale; FDPCU = flexor digitorum profundus caput ulnare; FCU = flexor carpi ulnaris; FDS = flexor digitorum superficialis; FCR = flexor carpi radialis; PT = pronator teres; PF 1 = pig forelimb 1; PF 2 = pig forelimb 2.

Comparison of Measurement Accuracy

The volumes of 18 muscles measured by drainage method, MRI VOI method and the other 2 conventional methods were shown in Table 3 (the results were the mean measurement of 6 times by 2 observers). The mean rank of the 3 methods with Kruskal-Wallis H test were 28.50, 29.06, and 24.94 respectively, χ^2 was 0.724, P value was 0.696, so no statistical difference existed among the 3 methods.

TABLE 3. The Average Volumes of 18 Muscles Measured by Three Methods and Its Actual Value

Volume (mm^3)	PF 1				PF 2			
	V_{act}	V_{VOI}	V_{sum}	V_{max}	V_{act}	V_{VOI}	V_{sum}	V_{max}
ECR	124.0	124.545	125.80	98.91	133.0	133.225	137.23	111.35
EDC	85.0	84.155	83.17	77.27	89.0	88.95	88.96	74.52
ECU	13.0	12.59	12.62	11.34	11.5	12.56	11.12	10.54
FDPCH	65.0	64.89	66.95	63.50	78.0	79.485	78.79	72.26
FDPCU	13.2	13.365	14.13	10.52	15.6	15.505	15.25	14.70
FCU	11.6	10.79	10.56	8.94	10.4	12.725	13.45	10.58
FDS	61.5	63.41	60.98	62.28	57.5	59.165	57.93	53.10
FCR	16.4	14.82	16.43	16.11	16.0	16.32	16.66	12.92
PT	20.2	18.78	20.10	18.25	24.6	24.215	25.14	24.57

ECR = extensor carpi radialis; EDC = extensor digitorum communis; ECU = extensor carpi ulnaris; FDPCH = flexor digitorum profundus caput humerale; FDPCU = flexor digitorum profundus caput ulnare; FCU = flexor carpi ulnaris; FDS = flexor digitorum superficialis; FCR = flexor carpi radialis; PT = pronator teres; PF 1 = pig forelimb 1; PF 2 = pig forelimb 2.

RMSE of 3 methods in 6 time points was 1.101 mL, 1.523 mL, and 8.99 mL respectively. The RMSE between VVOI and Vact was the smallest of all, less than the RMSE of Vsum and Vact or the RMSE of Vmax and Vact. These data showed the VOI method has the highest accuracy while the maximum section method with the lowest accuracy. Bland-Altman plot represented the minimum bias of −0.2219 between VVOI and Vact (the other 2 were −0.5424 and 5.2162), equivalent to a superior consistency (Figure 4).

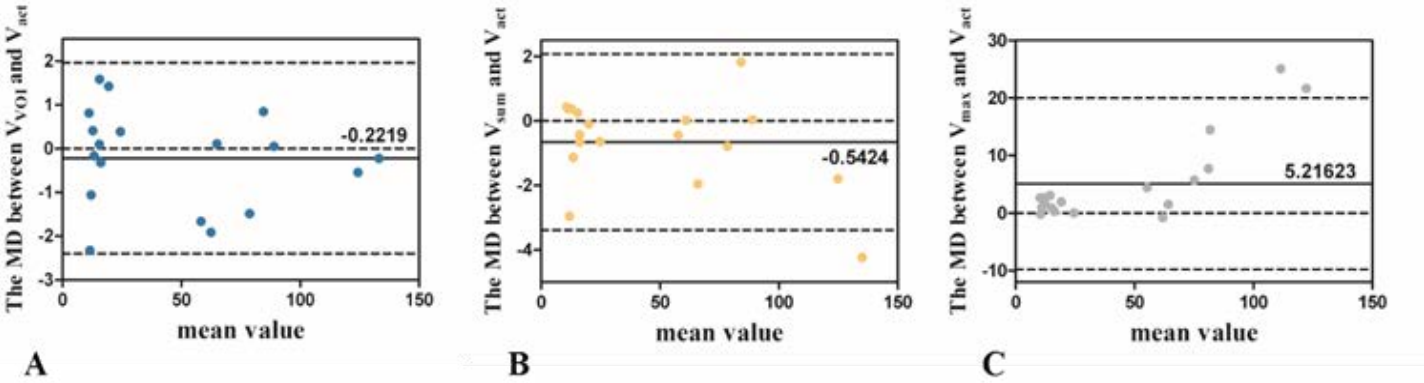

FIGURE 4. A Bland-Altman plot showed a comparison of the consistency of $V_{VOI,}$ V_{sum} and V_{max} to V_{act}. The bias between V_{VOI} and V_{act} was −0.2219, equivalent to a superior consistency.
V_{VOI} = The volume of MRI VOI method; V_{sum} = The volume of the summation method; V_{max} = The volume of the maximum section method; MD = mean value.

Measurement Consumption Time

The median consuming time to measure each muscle by the MRI VOI method, summation method, and the maximum section method was 1.07, 12.68 and 1.25 minutes respectively. The consume time of the 3 methods exhibited significant differences by Kruskal-Wallis H test. Pairwise Mann–Whitney U test and P value adjustment by FDR method exhibited the summation method taken the

longest time (P = 0.00061), nevertheless, MRI VOI method and the maximum section method had no statistical difference (P = 0.2692).

DISCUSSION

The current examination for evaluating skeletal muscle volumes, includes bioimpedance analysis (BIA), ultrasound, dual-energy x-ray absorptiometry (DXA), computed tomography (CT), and MRI.[26–30] Nevertheless, MRI has become the optimal method because of its non-invasiveness, high soft-tissue resolution, and 3-D configuration which could observe the morphological structure clearly and animatedly.[4,31]

In our study, the MRI VOI method was semi-automatic, merely to identify the interesting muscle and contour the enthesis of the muscle and slightly adjusted if the morphology was irregular. The internal slices were measured and delineated by the computer automatically based on the signal intensity, and the organization loss of the internal slices was compensated through interpolation calculation. Its segmentation speed was rapid, and the median consume time to measure each muscle in this study was 1.07 minutes, which was much shorter than the summation method volume (1.07 minutes vs. 12.68 minutes, P < 0.001). For another, the pick-up algorithm of VOI method was not only based on the interaction and transformation detecting techniques, but also the visual characteristics. It was seldom influenced by the image noise, so the method could be performed on conventional MRI images and does not require high-resolution scanning, which would have a wider application.

In this study 2 physicians completed the process independently 6 times, the Friedman test and ICC showed a high intra- and inter-reliability, and a good repeatability of volume measurements. What's more, compared with the summation method and the maximum section method, the VOI method has the smallest RMSE, which approximated to the actual values (RMSE of 3 methods was 1.101 mL, 1.523 mL, and 8.99 mL respectively).

The innovation of this research was that the accuracy of VOI method measurements was verified with the true muscle, which was more intuitive and credible. As the morphology and volume of the pig forelimb is similar to humans, using pig forelimbs in place of intravital human limbs could solve any ethical problems and reduce research costs.[1] In the drainage method, several high-resolution photos were taken horizontally and rechecked by 2 observers (the photos were amplified and viewed repeatedly), which was conducive to collate the readings, ensure the results more veritably, and avoid errors.

This current study has some limitations that should be considered. First, the sample capacity was low. Only 2 left forelimbs (18 skeletal muscles) from 2 live domestic pigs were included in the study, although each method was measured 6 times using 3 methods. Second, although the pig forelimbs were similar in shape and nomenclature to the human upper limbs, there were some differences inevitably. Third, at present the VOI method software was still semi-automatic, in the future, an automatic component analysis through artificial intelligence will be realized, which could reduce the working hours greatly.

CONCLUSION

In summary, the 3-D reconstructs of MRI VOI method semi-automatically was used to display the morphological structure of skeletal muscle. Compared with the real skeletal muscles, the VOI method has been verified to have great accuracy and high repeatability. Herein, this method can be employed as a clinical non-invasive evaluation tool for muscle atrophy such as sarcopenia, age-related degeneration, rotator cuff tears, or be used as an observation indicator in orthopedics and sports medicine.

REFERENCES

1. Santago AC, Plate JF, Shively CA, Register TC, Smith TL, Saul KR. Age-related structural changes in upper extremity muscle tissue in a nonhuman primate model. J Shoulder Elbow Surg 2015;24(10):1660–8. https://doi.org/10.1016/j.jse.2015.03.025.
2. Chi AS, Long SS, Zoga AC, Parker L, Morrison WB. Association of gluteus medius and minimus muscle atrophy and fall-related hip fracture in older individuals using computed tomography. J Comput Assist Tomogr 2016;40(2):238–42. Available at: https://www.ncbi.nlm.nih.gov/pubmed/26571058

3. Vidt ME, Daly M, Miller ME, Davis CC, Marsh AP, Saul KR. Characterizing upper limb muscle volume and strength in older adults: a comparison with young adults. J Biomech 2012;45(2):334–41. Available at: https://www.ncbi.nlm.nih.gov/pubmed/22047782
4. Li F, Laville A, Bonneau D, Laporte S, Skalli W. Study on cervical muscle volume by means of three-dimensional reconstruction. J Magn Reson Imaging 2014;39(6):1411–6. Available at: https://www.ncbi.nlm.nih.gov/pubmed/24123770
5. Scheibel M, Nikulka C, Dick A, Schroeder RJ, Popp AG, Haas NP. Structural integrity and clinical function of the subscapularis musculotendinous unit after arthroscopic and open shoulder stabilization. Am J Sports Med 2007;35(7):1153–61. Available at: https://www.ncbi.nlm.nih.gov/pubmed/17379917
6. Dufour AB, Hannan MT, Murabito JM, Kiel DP, McLean RR. Sarcopenia definitions considering body size and fat mass are associated with mobility limitations: the Framingham Study. J Gerontol A Biol Sci Med Sci 2013;68(2):168–74. Available at: https://www.ncbi.nlm.nih.gov/pubmed/22503991
7. Yoo YH, Kim HS, Lee YH, et al. Comparison of multi-echo dixon methods with volume interpolated breath-hold gradient echo magnetic resonance imaging in fat-signal fraction quantification of paravertebral muscle. Korean J Radiol 2015;16(5):1086–95. Available at: https://www.ncbi.nlm.nih.gov/pubmed/26357503
8. Maeda K, Shamoto H, Wakabayashi H, Akagi J. Sarcopenia is highly prevalent in older medical patients with mobility limitation. Nutr Clin Pract 2017;32(1):110–5. Available at: https://www.ncbi.nlm.nih.gov/pubmed/27881807
9. Liaghat B, Juul-Kristensen B, Frydendal T, Marie Larsen C, Sogaard K, Ilkka Tapio Salo A. Competitive swimmers with hypermobility have strength and fatigue deficits in shoulder medial rotation. J Electromyogr Kinesiol 2018;39:1–7. Available at: https://www.ncbi.nlm.nih.gov/pubmed/29353138
10. Gillet B, Begon M, Diger M, Berger-Vachon C, Rogowski I. Shoulder range of motion and strength in young competitive tennis players with and without history of shoulder problems. Phys Ther Sport 2018;31:22–8. Available at: https://www.ncbi.nlm.nih.gov/pubmed/29524909
11. Friesenbichler B, Item-Glatthorn JF, Neunstocklin F, Casartelli NC, Guilhem G, Maffiuletti NA. Differences in trunk and thigh muscle strength, endurance and thickness between elite sailors and non-sailors. Sports Biomech 2018;17(2):216–26. Available at: https://www.ncbi.nlm.nih.gov/pubmed/28632066
12. Pons C, Borotikar B, Garetier M, et al. Quantifying skeletal muscle volume and shape in humans using MRI: A systematic review of validity and reliability. PLoS On 2018;13(11):e0207847. Available at: https://www.ncbi.nlm.nih.gov/pubmed/30496308
13. Im HS, Alter KE, Brochard S, Pons C, Sheehan FT. In vivo pediatric shoulder muscle volumes and their relationship to 3D strength. J Biomech 2014;47(11):2730–7. Available at: https://www.ncbi.nlm.nih.gov/pubmed/24925254
14. Bolsterlee B, Finni T, D'Souza A, Eguchi J, Clarke EC, Herbert RD. Three-dimensional architecture of the whole human soleus muscle in vivo. Peer J 2018;6:e4610. Available at: https://www.ncbi.nlm.nih.gov/pubmed/29682414
15. Yoshiko A, Hioki M, Kanehira N, et al. Three-dimensional comparison of intramuscular fat content between young and old adults. BMC Med Imaging 2017;17(1):12. Available at: https://www.ncbi.nlm.nih.gov/pubmed/28183279
16. Yang X, Zhou Q, Zhang W, et al. The feasibility and preliminary application of deltoid muscle volume measurement using MR volume of interest method. Chinese J Radiol (China). 2018;52:687–91. DOI:10.3760/cma.j.issn.1005-1201.2018.09.008
17. Infantolino BW, Challis JH. Evaluation of a simple method for determining muscle volume in vivo. J Biomech 2016;49(9):1973–5. Available at: https://www.ncbi.nlm.nih.gov/pubmed/27156375
18. Tingart MJ, Apreleva M, Lehtinen JT, Capell B, Palmer WE, Warner JJ. Magnetic resonance imaging in quantitative analysis of rotator cuff muscle volume. Clin Orthop Relat Res 2003;(415):104–10. Available at: https://www.ncbi.nlm.nih.gov/pubmed/14612636
19. Eng CM, Abrams GD, Smallwood LR, Lieber RL, Ward SR. Muscle geometry affects accuracy of forearm volume determination by magnetic resonance imaging (MRI).

J Biomechanics 2007;40(14):3261–6. Available at: https://www.ncbi.nlm.nih.gov/pubmed/17521657

20. Fu C, Xia Y, Meng F, et al. MRI quantitative analysis of eccentric exercise-induced skeletal muscle injury in rats. Acad Radiol 2019. Available at: https://www.ncbi.nlm.nih.gov/pubmed/31300358
21. Bozkus H, Crawford NR, Chamberlain RH, et al. Comparative anatomy of the porcine and human thoracic spines with reference to thoracoscopic surgical techniques. Surg Endosc 2005; 19(12):1652–65. Available at: https://www.ncbi.nlm.nih.gov/pubmed/16211439
22. Galvez M, Montoya CE, Fuentes J, et al. Error measurement between anatomical porcine spine, ct images, and 3D printing. Acad Radiol 2019; Available at: https://www.ncbi.nlm.nih.gov/pubmed/31326309
23. Kneepkens AF, Badoux DM, MacDonald AA. Descriptive and comparative myology of the forelimb of the babirusa (Babyrousa babyrussa L. 1758). Anat Histol Embryol 1989;18(4):349–65. Available at: https://www.ncbi.nlm.nih.gov/pubmed/2624327
24. Raya SP, Udupa JK. Shape-based interpolation of multidimensional objects. IEEE Trans Med Imaging 1990;9(1):32–42. Available at: https://www.ncbi.nlm.nih.gov/pubmed/18222748
25. Chuang KS, Chen CY, Yuan LJ, Yeh CK. Shape-based grey-level image interpolation. Phys Med Biol 1999;44(6):1565–77. Available at: https://www.ncbi.nlm.nih.gov/pubmed/10498523
26. Ticinesi A, Meschi T, Narici MV, Lauretani F, Maggio M. Muscle ultrasound and sarcopenia in older individuals: a clinical perspective. J Am Med Dir Assoc 2017;18(4):290–300. Available at: https://www.ncbi.nlm.nih.gov/pubmed/28202349
27. Mueller N, Murthy S, Tainter CR, et al. Can sarcopenia quantified by ultrasound of the rectus femoris muscle predict adverse outcome of surgical intensive care unit patients as well as frailty? a prospective, observational cohort study. Ann Surg 2016;264(6):1116–24. Available at: https://www.ncbi.nlm.nih.gov/pubmed/26655919
28. Minetto MA, Caresio C, Menapace T, et al. Ultrasound-based detection of low muscle mass for diagnosis of sarcopenia in older adults. PM R 2016;8(5):453–62. Available at: https://www.ncbi.nlm.nih.gov/pubmed/26431809
29. Kim EY, Kim YS, Park I, et al. Evaluation of sarcopenia in small-cell lung cancer patients by routine chest CT. Support Care Cancer 2016;24(11):4721–6. Available at: https://www.ncbi.nlm.nih.gov/pubmed/27364150
30. Lee JS, Kim YS, Kim EY, Jin W. Prognostic significance of CT-determined sarcopenia in patients with advanced gastric cancer. PLoS One 2018;13(8):e0202700. Available at: https://www.ncbi.nlm.nih.gov/pubmed/30125312
31. Matsumura N, Oguro S, Okuda S, et al. Quantitative assessment of fatty infiltration and muscle volume of the rotator cuff muscles using 3-dimensional 2-point Dixon magnetic resonance imaging. J Shoulder Elbow Surg 2017;26(10):e309–e18. Available at: https://www.ncbi.nlm.nih.gov/pubmed/28495576

AUTHOR BIOGRAPHIES

Qing-Qing Zhou received a master's degree in radiology with Nanjing Medical University, Nanjing, China, in 2018. She is currently a radiologist working in the Radiology Department of The Affiliated Jiangning Hospital of Nanjing Medical University. Research interests include deep learning in skeletal muscle system and its applications.